Eur. Phys. J. B **51**, 209–213 (2006)
DOI: 10.1140/epjb/e2006-00214-x

THE EUROPEAN
PHYSICAL JOURNAL B

Fine structure effects and phase transition of Xe nanocrystals in Si

G. Faraci[1,a], A.R. Pennisi[1], and F. Zontone[2]

[1] Dipartimento di Fisica e Astronomia, Universitá di Catania; MATIS - Istituto Nazionale di Fisica della Materia, via Santa Sofia 64, 95123 Catania, Italy
[2] ESRF, European Synchrotron Research Facility, B.P. 220 38043 Grenoble Cedex, France

Received 30 January 2006 / Received in final form 7 April 2006
Published online 2 June 2006 – © EDP Sciences, Società Italiana di Fisica, Springer-Verlag 2006

Abstract. We report on an X-ray diffraction study performed on Xe agglomerates obtained by ion implantation in a Si matrix. At low temperature, Xe nano-crystals were formed in Si with different average sizes according to the preparation procedure. High resolution diffraction spectra were detected as a function of the temperature, in the range 15–300 K, showing evidence of fine structure effects in the growth mode of the Xe nanocrystals. We report the first experimental observation of fcc crystalline agglomerates with a lattice parameter expanded by the epitaxial condensation on the Si cavities, whereas for small agglomerates randomly oriented evidence of a contracted lattice was found. For these nanocrystals, a solid-to-liquid transition temperature, size dependent, was detected; above the transition temperature, a fluid phase was observed. Neither overpressurized clusters were detected at any temperature, nor preferential binary size distribution as reported for a metal matrix.

PACS. 61.10.Nz X-ray diffraction – 61.46.-w Nanoscale materials – 81.07.Ta Quantum dots

The confinement of rare gas clusters into a solid matrix can be easily obtained by ion implantation. In the last two decades, in fact, such agglomerates were observed [1–15] often in a pressurized solid phase, even at room temperature. For these observations, several techniques were adopted, including X-ray absorption spectroscopy [3–5], X-ray diffraction (XRD) [9,14], and transmission electron microscopy [12,13].

At temperatures lower than the solid rare gas melting point, the main features of these clusters appear well established when the host matrix is a metal [16]; in fact, nanocrystalline clusters of Kr in Al were observed by XRD with an apparent dual size distribution [14]; in contrast, mainly for Kr and Xe in a Si matrix, many controversial issues were recently raised. Actually, X-ray absorption fine structure (XAFS) investigation of as-implanted Kr in Si and Be did not show any evident XAFS structure [5] although clear evidence of clustering was obtained.

In the past, precipitates of Xe in a Si matrix were detected in crystal phase only after annealing [3,12]; this result was ascribed to the strong influence due to the substrate, since the implantation process at ambient temperature amorphizes a semiconductor but not a metal, and the thermal process favors the rare gas agglomeration. However, it is still uncertain whether a thermal treatment is necessary to produce cluster segregation and confinement in as-implanted semiconductors; in particular for Xe implanted in Si, around and beyond the melting point, there is contrast between the earlier interpretation of XAFS data [3] and recent XRD investigations [9]; in fact, at room temperature, the XAFS measurements showed a very low coordination interpreted as the coexistence of small solid clusters and large gas-like bubbles; in contrast, XRD data found evidence of a fluid phase with coordination 6 times larger. Additional questions are related to the evolution of the clusters [17], their phase transition as a function of the temperature, the size dependence of the physical parameters, the eventual coexistence of different phases and/or multiple cluster size distributions.

In more details, the most important questions which motivate a deep investigation of this topic concern: (i) whether solid overpressurized Xe bubbles are present, in a Si matrix, at temperatures larger than the solid Xe melting point; (ii) whether Xe clusters agglomerate with a preferential (dual) distribution; (iii) the differences induced by a thermal treatment of the Si matrix in the growth of the Xe nanocrystals.

For the previous reasons we revisited the Xe clustering in a silicon matrix, measuring high resolution XRD spectra as a function of the temperature. Clusters of 45

[a] e-mail: giuseppe.faraci@ct.infn.it

and 340 Å (in as-implanted silicon), 140 and 340 Å (in an annealed matrix) revealed the following surprising characteristics:

(i) fcc solid agglomerates in crystalline phase were found for temperature under the individual melting point. Fine structural effects were discovered in the Xe fcc diffraction pattern; in fact, in as-implanted samples, for spherical randomly oriented Xe clusters with radius $r = 22.5$ Å the influence of the surface tension $2\gamma/\mathrm{r}$ determined a lattice contraction; on the contrary, in annealed samples, for 70 Å clusters an expansion was discovered due to the epitaxial alignment induced by the Xe condensation on the Si matrix cavities. This is the first experimental observation of a strain contribution expanding the Xe lattice parameter up to the transition temperature;

(ii) in contrast with XAFS analysis, no overpressurized solid bubbles were detected at any temperature. In fact, above the melting point a fluid phase was always detected.
In contrast with the behaviour of Kr in Al, no dual or discrete-size distribution was observed in the annealed samples;

(iii) a fine structure of the (111) fcc peak was discovered, and the peak was deconvoluted in a triplet showing evidence of stacking faults;

(iv) the solid-to-liquid phase transition temperature was determined with a strong dependence on the cluster size;

(v) expansion of the lattice parameter was accurately observed as a function of the temperature, in each case.

In this letter we report the most important results obtained by XRD, confirmed by extensive measurements using transmission electron microscopy, small angle X-ray scattering and X-ray absorption spectroscopy which will be published in forthcoming papers.

Here, we compare high resolution X-ray diffraction spectra of two typical Xe/Si samples, the first implanted at high fluence (10^{17} at/cm^2 at 200 keV, annealed 1 h at 700 °C) labelled H_{an}, the second implanted at a lower fluence (10^{16} at/cm^2 at 100 keV, annealed 1 h at 700 °C), labelled L_{an}. The retained Xe dose checked by Rutherford back scattering was respectively 4.8×10^{16} and 10^{16} at/cm^2; other two samples, not annealed, were prepared as above, but with comparable doses 5×10^{16} at/cm^2. The first H_{as}, as implanted, at high fluence; the second L_{as} at low fluence and somewhat larger current (corresponding to a substrate temperature of about 150 °C). In these conditions the implantation profile has a Gaussian shape centered at about 50–100 nm below the matrix surface.

The experiments were performed at the European Synchrotron Radiation Facility, on the ID10A station of the Troika beamline, in the range of temperature $15–300 \pm 0.1$ K, at a photon energy 8.079 keV (wavelength $\lambda = 1.535$ Å). The samples were mounted in a closed-loop displex cryostat sitting on the ID10A four-circles diffractometer operating in horizontal scattering geometry. Scattering curves as a function of the temperature down to 15 K have been collected by θ_s scans, θ_s being the scattering angle, with the sample in grazing incidence geometry; this geometry allows to enhance the signal from the xenon clusters in the thin layer beneath the surface. The information obtainable from scattering measurements concerns the peak position, intensity and shape. The experimental resolution $\Delta Q/Q$ is smaller than 0.006 (Q being the momentum transfer, $Q = 4\pi \sin\theta_s/\lambda$).

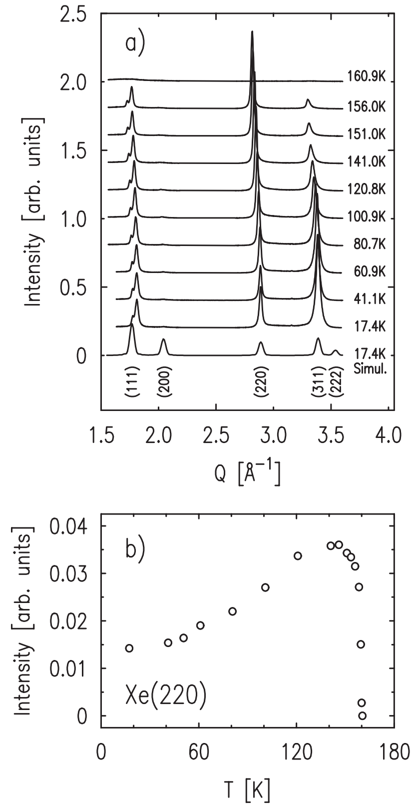

Fig. 1. (a) Scattering intensity profiles of the sample H_{an} with $D = 340$ Å at different temperatures, showing well resolved fcc diffraction peaks from Xe. Curves have been vertically shifted for clarity. The simulated fcc pattern for randomly oriented 340 Å clusters at 17.4 K is also shown. (b) Integrated intensity of the Xe(220) reflection ($Q = 2.9$ Å^{-1}) as a function of the temperature showing the sharp melting transition.

An extensive description of the experimental arrangement can be found in reference [18].

In Figures 1 and 2, the XRD spectra of the samples H_{an} and H_{as} are displayed for different temperatures; three main fcc peaks can be easily identified with small residual background reflections from the Si matrix and the Be window of the cryostat; after few months, the experiments were repeated at a different photon energy, with a very nice reproducibility. Similar spectra were obtained for the other samples.

As clearly visible in the figures, all the peaks and their evolution as a function of the temperature have revealed, at low temperature, ensembles of solid Xe clusters in nanocrystalline phase, perfectly matching the fcc configuration. From the peaks, fitted by a pseudo Voight profile, the average cluster size D can be easily determined by

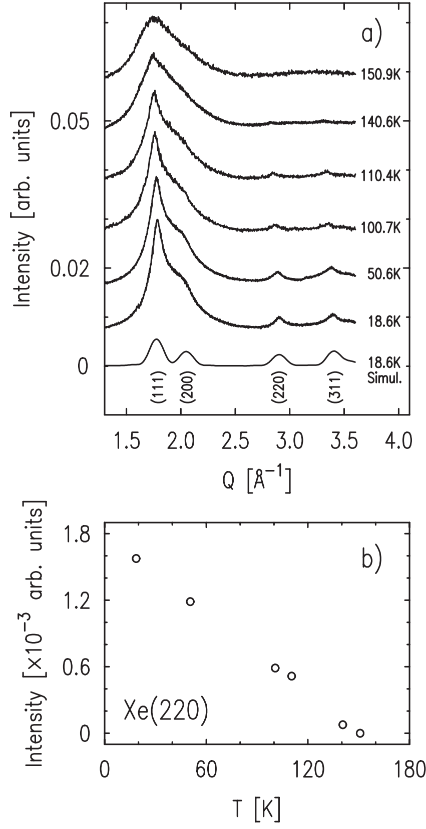

Fig. 2. (a) Scattering intensity profiles of the sample H_{as} with $D = 45$ Å at different temperatures, showing broad diffraction peaks from Xe. Curves have been vertically shifted for clarity. The simulated fcc pattern for randomly oriented 45 Å clusters at 18.6 K is also shown. (b) Integrated intensity of the Xe(220) reflection ($Q = 2.9$ Å^{-1}) as a function of the temperature showing a broad melting transition.

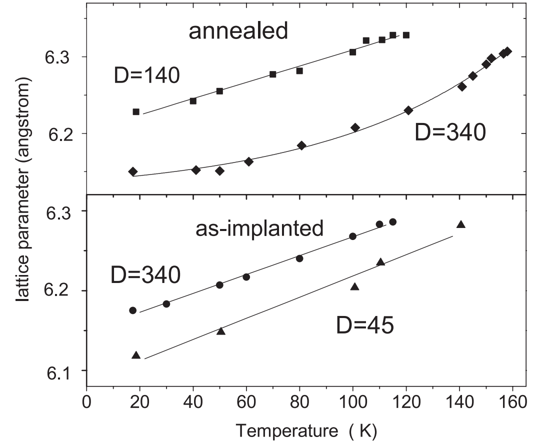

Fig. 3. Temperature dependence of the lattice parameter of Xe nanocrystals with the specified size. The size of the symbols gives the error bar for each point. The highest temperature in each plot indicates the phase transition limit. The lines are a guide to the eye.

the Scherrer formula $D = \frac{\lambda}{\beta \cos \theta_s}$ where λ is the radiation wavelength and β the full width at half maximum of the peak located at $2\theta_s$.

As well known, being our Xe agglomerates polycrystalline, the Scherrer formula gives the average nanocrystal size of the entire distribution; a more detailed analysis of the diffraction peaks could derive also the eventual presence of strain.

For the above mentioned samples we obtain the following average sizes of the Xe nano-crystals:

for H_{an}, $D = 340$ Å; for L_{an}, $D = 140$ Å;
for H_{as}, $D = 45$ Å; for L_{as}, $D = 340$ Å.

The obtained cluster size of the annealed samples is due to the different retained dose. In the as-implanted cases the higher size is related to the higher substrate temperature, not high enough however to avoid the amorphization of the matrix. For all the samples, it can be excluded the presence of binary size distributions, because the shape of the peaks could not be deconvoluted in two components having different width. For comparison in the figures a simulated spectrum at low temperature for a spherical fcc Xe cluster of the same size is reported, with the corresponding intense contributions for the (111), (200), (220) and (311) peaks. The comparison with the corresponding simulations shows evidence of polidisperse agglomerates with a spread evaluated, for the annealed samples, in the order of about 20%. An obvious intensity mismatch is the signature of strong preferred orientation effects with epitaxial alignment with the matrix induced by the thermal treatment in the annealed samples.

The angular positions of the most intense peaks (220) and (311) can been accurately determined; they demonstrate the contribution of Xe fcc nanocrystals with the mentioned sizes expanding with increasing temperature; they also permit a precise localization of the solid-to-liquid transition temperature.

In Figure 3 we show the temperature dependence of the lattice parameter resulting from fitting the peak positions of the diffraction lines. By monitoring the integrated intensities, the correspondent solid-to-liquid transition temperature could be easily determined as well.

We find that in the annealed samples the larger nanocrystals ($D = 340$ Å) melt at $T = 157.5 \pm 2.5$ K, the smallest ($D = 140$ Å) at $T = 117.5 \pm 2.5$ K; in the as-implanted samples, for $D = 340$ Å, $T = 117.5 \pm 2.5$ K, for $D = 45$ Å, $T = 130 \pm 10$ K. The range in the temperature indicates the presence of narrow hysteresis effects. These values compare with the bulk Xe crystal melting point (161.4 K) at ambient pressure.

Above the transition temperature no detectable diffraction lines could be revealed and only a smooth intensity distribution with very broad features is left, confirming the absence of whatever small cluster in solid phase.

Note also that for the annealed sample with $D = 340$ Å, the lattice parameter is nearly constant at low temperature, with a value (6.15 ± 0.01 Å) between that of bulk xenon at 0 K (6.132 Å), and the measured one of bulk Xe at 50 K (6.166 Å) [19]; near the melting point,

this value reaches 6.307 ± 0.005 Å, somewhat less than the value 6.346 Å, deduced from the molar volume predicted by the equation of state for bulk Xe (38.49 cm^3/mol) [20].

For the as-implanted sample having smaller clusters (45 Å), the lattice constant at low temperature is 6.118 ± 0.005 Å. As the temperature increases a linear lattice expansion is observed and the lattice constant reaches the value 6.283 ± 0.007 Å, at 135 K well below that of bulk Xe [20,21].

We discuss now the obtained results, distinguishing the as-implanted samples from the annealed ones.

In the H_{as} sample ($D = 45$ Å), at the lowest temperature, the intensity profile shows very broad peaks at the typical fcc positions of a Xe nanocrystal; as the temperature increases, the diffraction lines shift towards low Q because of the expansion of the unit cell. The line broadening reflects both the size spread of the Xe agglomerates and the intrinsic single size linewidth. Of course, in the average of different sizes, weighting factors proportional to the cluster volume play an important role so that small nanocrystals or diffuse Xe agglomerates have a minor relative intensity. The spectra of as-implanted samples show also evidence of a disordered phase even at the lowest temperature, also due to Xe atoms in fluid phase, in a kind of network of clusters of various size and of single atoms generated by the implantation process. The polidisperse size of the condensed phase does not allow an unique state and at low temperature only clusters of a few tens of Å can present the fcc crystal phase. Both the as-implanted samples show a large melting transition, corresponding to a broad size distribution with a melting at constant volume; here, smaller clusters have smaller lattice parameter because of the effects of the surface tension $T = 4\gamma/D$. This tension can be evaluated: assuming in Si $\gamma = 0.625$ J/m^2 [12] we obtain a pressure $T = 0.48$ GPa, producing the lattice parameter contraction of 0.06 Å between the two sizes. As expected, a higher transition temperature corresponds to a smaller lattice parameter.

In contrast with the as-implanted samples, in the annealed ones we obtain well defined and narrower diffraction lines typical of larger fcc nanocrystals. This confirms that the annealing favors the agglomeration of larger Xe clusters, corroborated by the sharp melting transition with a negligible contribution of surface tension, because of the larger size. The higher intensity of peaks (220) and (311) is also the signature of strong preferred orientation effects induced by the Si matrix, with the xenon epitaxially condensated on the wall of the Si cavities. This condensation explains why smaller clusters have larger lattice parameters, here dramatically influenced by the Si(100) matrix; we recall that the annealing process has produced the regrowth of the matrix amorphized by the implantation. Therefore, in polycrystalline Si cavities, Xe condenses with a lattice parameter strongly influenced by the lattice mismatch between Si and Xe. Here too, a higher transition temperature corresponds to a smaller lattice parameter.

In both annealed and as implanted samples we obtain (Fig. 3) a Xe lattice parameter expanding as a function of the temperature; from these data we can then exclude any compressed or overpressurized phase; such phase, if present, should increase the melting temperature, as observed for metal matrices; on the contrary, the Xe solid phase dissolves in a fluid phase already below the bulk limit. Taking into account that crystalline Si is elastically a quite stiff material and can withstand large pressures, we conclude that the observed sharp melting transition indicates that the volume available for Xe clusters in the annealed cases is large enough for allowing Xe expansion without any overpressure.

In the as-implanted samples the shape of the first diffraction peaks indicates the presence of a dominating "amorphous" background and suggests the presence of a large amount of Xe in very small disordered aggregates.

As a matter of fact, these results were confirmed by wide scans taken with an imaging plate, at low temperature. The imaging plate shows for as-implanted samples uniform fcc Debye-Scherrer rings due to randomly oriented Xe clusters; for annealed samples, very textured diffraction lines are present due to strong preferred orientation effects, and in addition the (111) line is clearly observed possessing a fine structure where the main fcc reflection peak has smaller satellites or shoulders at high and low Q side. This fact already reported in the literature is related to stacking faults [22].

Our results confirm that the mechanical equilibrium of Xe nano aggregates cannot be described only by surface tension, in agreement with a recent investigation on the coalescence of Xe nano particles [17].

In conclusion, we reported the first experimental observation about fine structural modifications in the lattice parameter of fcc Xe nanocrystals in Si, according to the growth morphology. In smaller clusters in fact, we found a lattice parameter expanded by the epitaxial condensation on the *ordered* silicon matrix, whereas lattice contraction is observed for a random orientation of the nanocrystals in the *amorphous* silicon matrix; evidence of size dependent solid-to-liquid phase transition was also pointed out, clarifying the thermodynamical behavior of the Xe aggregates in a semiconductor matrix. Overpressurized phases have been disproved.

The authors are grateful to ESRF staff for the excellent collaboration; thanks are also due to F. D'Acapito for helpful discussions.

References

1. A. vom Felde, J. Fink, Th. Müller-Heinzerling, J. Pflüger, B. Scheerer, G. Linker, D. Kaletta, Phys. Rev. Lett. **53**, 922 (1984)
2. E. Fleischer, M.G. Norton, Heterog. Chem. Rev. **3**, 171 (1966)
3. G. Faraci, A.R. Pennisi, A. Terrasi, S. Mobilio, Phys. Rev. B **38**, 13468 (1988); G. Faraci, in *Fundamental Aspects of Inert Gases in Solids, Nato ASI series*, edited by S.E. Donnelly, J.H. Evans (1991), Vol. 279, p. 251
4. G. Faraci, S. La Rosa, A.R. Pennisi, S. Mobilio, G. Tourillon, Phys. Rev. B **43**, 9962 (1991)

5. G. Faraci, A.R. Pennisi, J.L. Hazemann, Phys. Rev. B **56**, 12553 (1997)
6. A. Polian, J.P. Itie, E. Dartyge, A. Fontaine, G. Tourillon, Phys. Rev. B **39**, 3369 (1989)
7. C.J. Rossouw, S.E. Donnelly, Phys. Rev. Lett. **55**, 2960 (1985)
8. R.C. Birtcher, W. Jaeger, J. Nucl. Mater. **135**, 274 (1985); R.C. Birtcher, in *Fundamental Aspects of Inert Gases in Solids, Nato ASI series*, edited by S.E. Donnelly, J.H. Evans (1991), Vol. 279, p. 133
9. F. Zontone, F. D'Acapito, G. Faraci, A.R. Pennisi, Eur. Phys. J. B **19**, 501 (2001)
10. M. Wittmer, J. Roth, J.W. Mayer, J. Appl. Phys. **49**, 5207 (1978)
11. A. Luukkainen, J. Keinonen, A. Erola, Phys. Rev. B **32**, 4814 (1985)
12. C. Templier, B. Boubeker, H. Garem, E.L. Mathe', J.C. Desoyer, Phys. Stat. Sol. a **92**, 511 (1985)
13. C. Templier, H. Garem, J.P. Riviere, Phil. Mag. A **53**, 667 (1986)
14. H.H. Andersen, J. Bohr, A. Johansen, E. Johnson, L. Sarholt-Kristensen, V. Surganov, Phys. Rev. Lett. **59**, 1589 (1987)
15. P. Revesz, M. Wittmer, J. Roth, J.W. Mayer, J. Appl. Phys. **49**, 5199 (1978)
16. E.L. Fleischer, M. Grant Norton, Heter. Chem. Rev. **3**, 171 (1996)
17. R.C. Birtcher, S.E. Donnelly, M. Song, K. Furuya, K. Mitsuishi, C.W. Allen, Phys. Rev. Lett. **83**, 1617 (1999)
18. G. Grübel, F. Zontone, J. Alloys and Comp. **362**, 3 (2004)
19. D. Richard Sears, H.P. Klug, J. Chem. Phys. **37**, 3002 (1962)
20. M.S. Anderson, C.A. Swenson, J. Chem. Phys. **36**, 145 (1975)
21. Ph. Buffat, J.P. Borel, Phys. Rev. A **13**, 2287 (1976)
22. H. Cynn, C.S. Yoo, B. Baer, V. Iota-Herbel, A.K. McMahan, M. Nicol, S. Carlson, Phys. Rev. Lett. **86**, 4552 (2001); D. Errandonea, B. Schwager, R. Boehler, M. Ross, Phys. Rev. B **65**, 214110 (2002)